Solid State Ionics 51 (1992) 297–303
North-Holland

SOLID
STATE
IONICS

Anion-excess fluorite type solid solutions MF_2–NdF_3 and MF_2–UF_4 (M = Ca, Ba): conductivity and EXAFS spectroscopic study

D. Grandjean, T. Challier, D.J. Jones and P. Vitse

Laboratoire des Agrégats Moléculaires et Matériaux Inorganiques, URA CNRS 79, Université Montpellier II, 34095 Montpellier Cedex 5, France

Received 2 December 1991; accepted for publication 7 February 1992

The evolution of the electrical properties of fluorite-type solid solutions $Ba_{1-x}U_xF_{2+2x}$ ($0<x<0.24$), $Ba_{1-x}Nd_xF_{2+x}$ ($0<x<0.30$) and $Ca_{1-x}Nd_xF_{2+x}$ ($0<x<0.30$), with temperature up to 800°C has been investigated, and the conductivity of the solid solutions has been studied as a function of their composition and the nature of the aliovalent metal ion. At 800°C, the conductivity of all the solid solutions reaches a maximum value of ca. 10 Sm^{-1}. An EXAFS spectroscopic study of the $Ba_{1-x}U_xF_{2+2x}$ system has allowed the definition of the local environment of uranium in solid solutions containing up to 25 mol% of the element. In this structure, uranium is surrounded by 9 fluorine atoms located at 2.30 ± 0.01 Å, 8 barium and 4 uranium atoms at 4.36 ± 0.02 Å. Attempts are made to correlate structural and transport data.

1. Introduction

The introduction of aliovalent cations into fluorite type structures in the systems MF_2–$M'F_n$ ($M'F_n = NdF_3$, UF_4), by the generation of vacancies and/or interstitial sites confers a particular structure to these materials allowing them to show high conductivities. In fact, among solid electrolytes, fluorite type conductors have become a subject of study of considerable importance. Some fluoride ion conductors such as $Pb_{1-x}Bi_xF_{2+2x}$ [1–6], demonstrate sufficiently good electrical properties that they are already used as specific electrodes, solid batteries or gas detectors. Although the conductivities of the solid solutions $Ca_{1-x}Y_xF_{2+x}$, [7,8], $Sr_{1-x}In_xF_{2+x}$ [3], $Sr_{1-x}Bi_xF_{2+x}$ [3], $Ba_{1-x}La_xLa_xF_{2+x}$ [9–12], $Ba_{1-x}In_xF_{2+x}$ [13], $Ba_{1-x}Bi_xF_{2+x}$ [13], $Pb_{1-x}Bi_xF_{2+x}$ [2–4,14], $Pb_{1-x}In_xF_{2+x}$ [3], $Pb_{1-x}Ta_xF_{2+x}$ [14] are now well known, the electrical properties of the solid solutions $Ca_{1-x}Nd_xF_{2+x}$, $Ba_{1-x}Nd_xF_{2+x}$ and $Ba_{1-x}U_xF_{2+2x}$ have not been extensively studied at high temperature. At the present time, the conductivity of the solid solution $Ba_{1-x}Nd_xF_{2+x}$ has only been seriously investigated up to 200°C [15]. When we started our work, no systematic study of the conductivity of the solid solution $Ca_{1-x}Nd_xF_{2+x}$, had been reported, and the study of the electrical properties of the solid solution $Ba_{1-x}U_xF_{2+2x}$ [16] carried out at high temperature (up to 800°C), was limited to the low concentration range in UF_4 ($x<0.125$). The first part of this work was to investigate the evolution of the electrical properties of fluorite-type solid solutions $Ba_{1-x}U_xF_{2+2x}$, $Ba_{1-x}Nd_xF_{2+2x}$ and $Ca_{1-x}Nd_xF_{2+x}$ with temperature up to 800°C.

Since the first crystallographic studies based on the anion excess solid solutions UO_{2+x} [17–19] and $Ca_{1-x}Y_xF_{2+x}$ [20,21], showing the presence of defect clusters in this type of compound, a great number of other experimental studies using various techniques such as optical spectroscopy [22], ESR, EPR [11], NMR [11] and recently EXAFS [23,24], have allowed the demonstration of the presence of defect aggregates in numerous fluorite type solid solutions. Among those studied in the present work, $Ca_{1-x}Nd_xF_{2+x}$ has been studied by EXAFS spectroscopy [23], and the structure of $Ba_{1-x}U_xF_{2+2x}$ investigated by powder neutron diffraction [25,26]. We present here an EXAFS spectroscopic study of various compositions of the solid solution $Ba_{1-x}U_xF_{2+2x}$ in an effort to correlate the evolution of high temperature conductivity properties with the

structural properties in the solid solutions $Ca_{1-x}Nd_xF_{2+x}$, $Ba_{1-x}Nd_xF_{2+x}$ and $Ba_{1-x}U_xF_{2+2x}$.

2. Experimental

2.1. Synthesis

NdF_3 and UF_4 (>99%) were supplied by Comurhex Industries. CaF_2 and BaF_2 (LABOSI, 99.5%) were dried at 700°C for 24 h before use. Solid solutions $Ba_{1-x}U_xF_{2+2x}$, $Ba_{1-x}Nd_xF_{2+x}$ and $Ca_{1-x}Nd_xF_{2+x}$ were prepared by direct reaction of the metal fluorides at high temperature. After prolonged grinding of the powders in appropriate stoichiometries, they were pressed into discs of ca. 99.5% compacity, placed in a bomb, and heated for 24 h at 900°C for the $Ba_{1-x}Nd_xF_{2+x}$ and $Ca_{1-x}Nd_xF_{2+x}$ systems, 850°C for $Ba_{1-x}U_xF_{2+2x}$, under a constant stream of argon (1 ℓ/h). The various compositions of the individual solid solutions extended from 5% to the maximum concentration permitted by the phase diagram for $Ca_{1-x}Nd_xF_{2+x}$ and $Ba_{1-x}U_xF_{2+2x}$ (x_L, the limiting value of x at 900°C, is 0.30 [27] and 0.25 [28,29] respectively), and up to $Ba_{0.7}Nd_{0.3}F_{2.3}$ ($x_L=0.50$) [30]. All phases were characterised at room temperature by powder X-ray diffraction (Cu Kα radiation).

2.2. Conductivity measurements

ac impedance measurements were carried out on discs of compacted polycrystalline powders held between platinum electrodes, between 0.05 and 13000 kHz on an HP 4192 A instrument in the temperature range 200–800°C (measurement every 50°C between 200–450°C and every 10°C thereafter). The conductivity cell was maintained under dynamic vacuum (10^{-1} Pa).

2.3. X-ray absorption spectroscopy

EXAFS spectra were recorded at the uranium L_{III} edge (17164 eV) on station 9.2 at the SRS (Daresbury Laboratory, Cheshire, U.K.), operating under beam conditions of 2 GeV, 200 mA. The spectrometer was equipped with a Si (200) double crystal monochromator slightly detuned for harmonic rejection. Spectra were recorded from, in general, 100 eV before the edge to 900 eV after, in a series of step-sizes and counting times within energy regions corresponding to pre-edge, edge, near post-edge and far post-edge. The spectrometer was energy-calibrated before scanning using a 20 μm foil of zirconium having an absorption edge ($E_0=17998$ eV) close to that of uranium.

Powdered samples were examined spectroscopically as paraffin oil mulls pressed between the parafilm windows of stainless steel holders, producing an edge jump $\Delta\mu x$ of ca. 1. All spectra were recorded at 77 K using a cold finger cryostat. Ionisation chambers I_0 and I_T were filled with argon/helium and krypton/helium mixtures respectively: I_0 341 Torr argon, I_T 198 Torr krypton; the complement of helium was added in each case to bring the total pressure to 1 atm.

All data analysis was performed using the routines developed by Michalowicz [31] with a linear pre-edge function and a high order (5–6th) polynomial for normalization/background removal in the $\mu_{1,exp}-\mu_{0,exp}$ convention. Fourier transformation (Hamming window) was carried out over the range 2.5–15 $Å^{-1}$. Curve fitting was performed in reciprocal space on Fourier-filtered spectrum using phase and amplitude functions derived from UF_4. The EXAFS spectra of UF_4 were checked for compatibility with published bond length and coordination data obtained from X-ray diffraction [32,33].

3. Results and discussion

3.1. X-ray diffraction

All X-ray diffractograms could be indexed in the cubic system. The cell parameter, a, was in each case a linear function of the composition of the solid solution. In the case of $Ba_{1-x}U_xF_{2+2x}$ and $Ba_{1-x}Nd_xF_{2+x}$, a decreases regularly from 6.1992 Å (BaF_2) to 6.1067 Å in $Ba_{0.79}U_{0.21}F_{2.42}$, and to 6.1167 Å in $Ba_{0.7}Nd_{0.3}F_{2.3}$. Expansion of the fluorite unit cell is observed on formation of solid solutions of CaF_2 with NdF_3, with a regular increase in lattice parameter from 5.4647 Å (CaF_2) to 5.5568 Å for $Ca_{0.7}Nd_{0.3}F_{2.3}$. These values are generally in good agreement with literature values [28,29,34].

3.2. Conductivity measurements

The variation of the conductivity of the solid solutions $Ba_{1-x}U_xF_{2+2x}$, $Ba_{1-x}Nd_xF_{2+x}$ and $Ca_{1-x}Nd_xF_{2+x}$ with temperature, throughout the concentration range 5–24% for the first system and 5–30% for the latter two, is shown in fig. 1. In all cases but one ($Ca_{0.95}Nd_{0.5}F_{2.05}$), the conductivity of the solid solution is higher than that of undoped CaF_2 or BaF_2, the conductivities of which are respectively 3.4×10^{-5} and 1.5×10^{-4} Sm^{-1} at 400°C, increasing to 0.8 and 0.6 Sm^{-1} at 800°C. These values agree with those reported previously [16,35]. For the solid solutions, the simplest behaviour is observed for the $Ba_{1-x}Nd_xF_{2+x}$ system, where the spread of conductivities at temperatures below ca. 500°C converges to a conductivity, for all compositions, of ca. 10 Sm^{-1}, representing a 15-fold increase compared with that of undoped BaF_2. For $Ca_{1-x}Nd_xF_{2+x}$, a systematic augmentation in conductivity is observed on increasing the concentration of NdF_3 in the CaF_2 matrix between 10–30%, at a given temperature. A tendency towards convergence above 550°C is observed, less pronounced than for $Ba_{1-x}Nd_xF_{2+x}$. The greatest overall gain in conductivity is observed for $Ba_{1-x}U_xF_{2+2x}$ where, at 700°C for example, the increase is > 100-fold.

All three systems demonstrate linear behaviour up to ca. 400°C, above which temperature a succession of regions is observed, punctuated by points of inflexion. The variation in activation energy associated with these three regions can be interpreted in terms of different modes of conduction which are adopted as the temperature increases [36].

The dependence of the conductivity on the composition of the solid solution is better seen in fig. 2, where the conductivity at 450°C is plotted as a function of the dopant concentration, x. Two types of behaviour are apparent from these curves, a first for the systems $Ba_{1-x}U_xF_{2+2x}$ and $Ba_{1-x}Nd_xF_{2+x}$, the second for the solid solution $Ca_{1-x}Nd_xF_{2+x}$. The first is characterised by a rapid increase in conductivity, followed by a region showing more moderate enhancement. The change in slope occurs at x ca. 0.10 for $Ba_{1-x}U_xF_{2+2x}$ and x ca. 0.05 in the case of $Ba_{1-x}Nd_xF_{2+x}$. The activation energies vary in an inverse fashion to the logarithm of the conductivity (high activation energy initially 1.2 eV decreasing to

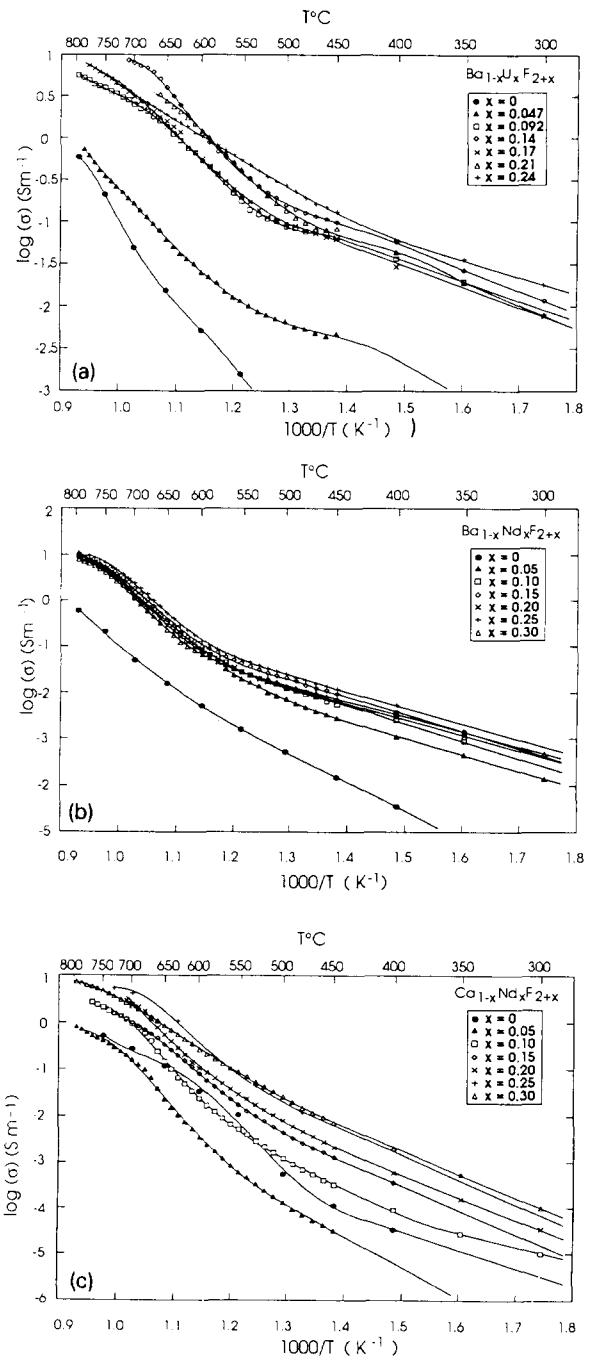

Fig. 1. Temperature dependence of the conductivity for the solid solutions: (a) $Ba_{1-x}U_xF_{2+2x}$ $0<x<0.24$; (b) $Ba_{1-x}Nd_xF_{2+x}$ $0<x<0.30$; (c) $Ca_{1-x}Nd_xF_{2+x}$ $0<x<0.30$.

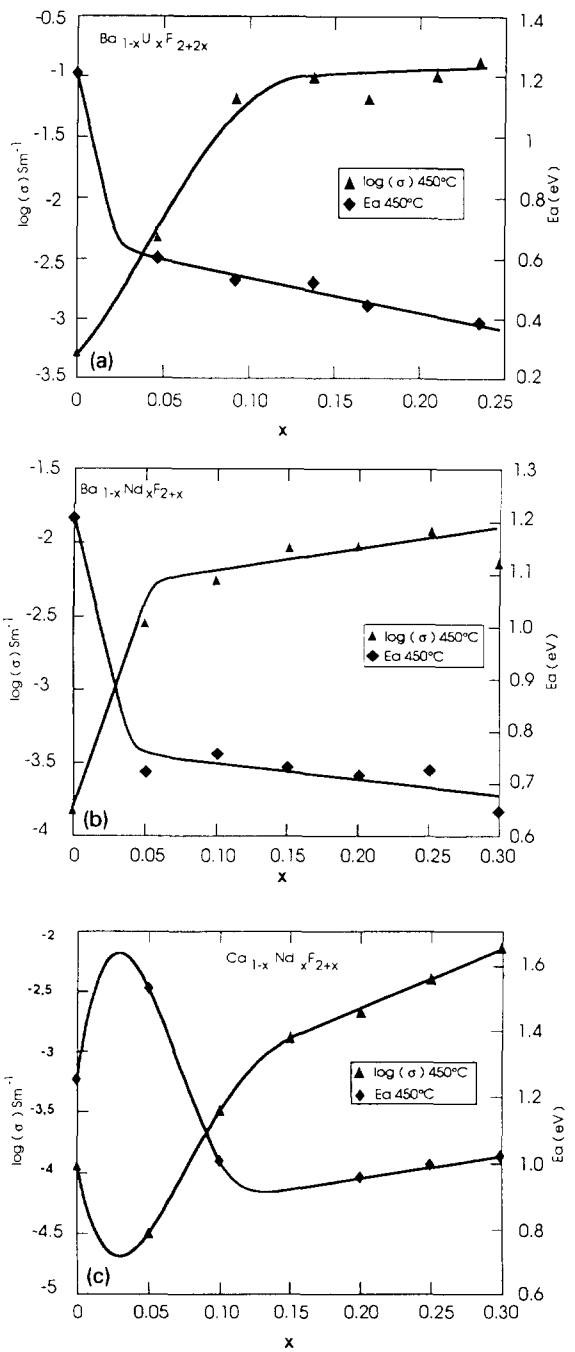

Fig. 2. Isotherm of the conductivity and activation energy (E_a) of (a) $Ba_{1-x}U_xF_{2+2x}$ $0<x<0.24$; (b) $Ba_{1-x}Nd_xF_{2+x}$ $0<x<0.30$; (c) $Ca_{1-x}Nd_xF_{2+x}$ $0<x<0.30$ as a function of the dopant concentration x.

0.7 eV in the case of $Ba_{1-x}Nd_xF_{2+x}$ and to 0.4 eV for $Ba_{1-x}U_xF_{2+2x}$.

Other conductivity data on these two systems have been reported [16,37]. Thus measurements on single crystals in the $Ba_{1-x}U_xF_{2+2x}$ solid solution [16] over composition ($x_L<0.125$) and temperature (500–900°C) ranges more restricted than those given here agree with the general appearance of the conductivity–composition isotherms. However, as expected, the individual values of the conductivity of the single crystals are higher than the corresponding measurements in the present study, performed on pressed powders. Electrical properties of the $Ba_{1-x}Nd_xF_{2+x}$ solid solution [37] have been studied over the concentration range $x_L=0$–0.32, but measurements were limited to an isotherm at 220°C. The values at this temperature are in reasonable agreement with those reported here, but the shape of isotherm is different. Furthermore, an isotherm similar to that given in fig. 2b for this solid solution has been reported previously for the $Ba_{1-x}La_xF_{2+x}$ system [9–12].

The second type of dependence of the conductivity on composition is displayed by $Ca_{1-x}Nd_xF_{2+x}$, where a minimum value of the conductivity is seen at x_L ca. 0.03 at all temperatures. This minimum was also observed in a recent study [35] published whilst the present work was already underway, although linear behaviour over the temperature range (300–1000 K) was observed.

3.3. X-ray absorption spectroscopy

The Fourier transformed (FT) EXAFS of uranium tetrafluoride contains two principal peaks at 184 Å and 4.34 Å resulting from backscattering from fluoride and uranium atoms. Filtering over these maxima and inverse Fourier transformation allowed extraction of the phase and amplitude functions using the crystallographically derived uranium environment [32,33] of 8 fluorine atoms at 2.278 ± 0.034 Å and 8 uranium atoms at 4.508 ± 0.042 Å.

Background subtracted and normalised EXAFS spectra and the corresponding Fourier transforms of typical solid solutions $Ba_{0.95}U_{0.05}F_{2.10}$ and $Ba_{0.79}U_{0.21}F_{2.42}$ are reproduced in fig. 3. Two types of curve can be observed according to the values of x:

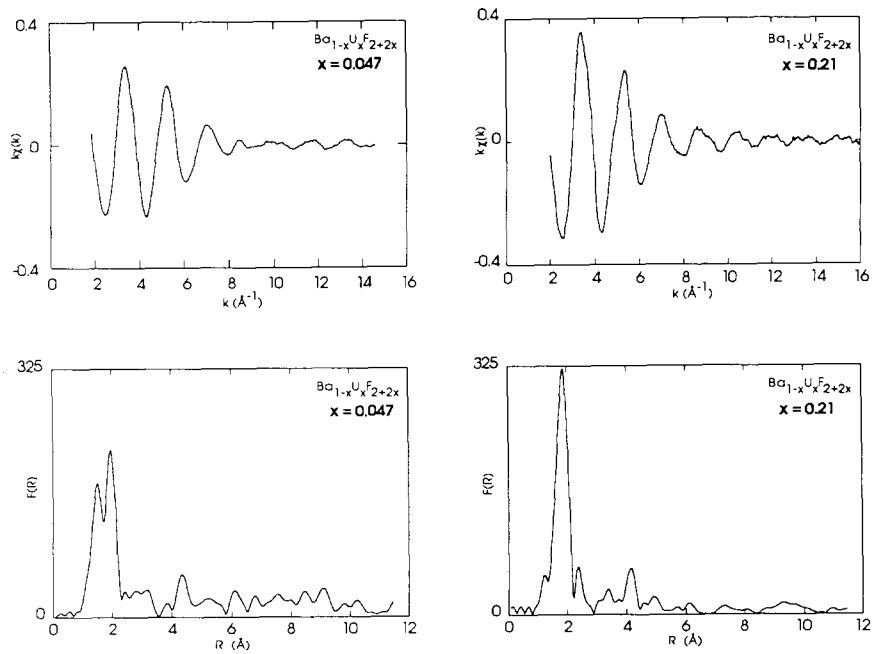

Fig. 3. EXAFS spectra and corresponding Fourier transforms of typical solid solutions $Ba_{0.95}U_{0.05}F_{2.10}$ and $Ba_{0.79}U_{0.21}F_{2.42}$.

(i) The compositions above $x=0.17$, all showing two well defined peaks of different intensity. The more intense, at ca. 1.9 Å before phase correction, can be attributed to a light atom shell, while the second at ca. 4.1 Å before phase correction, of lower intensity, results from a heavy atom shell located in the cationic sites.

(ii) The compositions below $x=0.14$, for which the first peak is split into 2 maxima while the second observed previously at longer distance is absent. This phenomenon, resulting from the absence of long range order with respect to uranium atoms in these samples, limits the useful information to the first shell of atoms. $Ba_{0.79}U_{0.21}F_{2.42}$, was used to derive a first structural model which could be applied as such, or modified as necessary to the other compositions. In this solid solution of lattice parameter $a=6.1161$ Å, the distances U–F and U–U expected by calculation (uranium located in the barium site) are 2.65 and 4.33 Å respectively.

The radial distribution function corresponding to the first coordination shell contains only one type of atoms. Curve fitting led to a number of neighbouring atoms close to 9, and a distance U–F ca. 2.30 ± 0.01 Å. The second peak of the FT corresponds to the second shell of atoms which could result from contributions from two types of metal ions, uranium and barium. The results of curve fitting to the experimental EXAFS showed 8 barium and 4 uranium atoms, all located at 4.36 ± 0.02 Å from the uranium absorber. Without any constraint, the nearest neighbor number U + Ba remained very close to 12, which is the expected coordination number for heavy atoms in a fluorite type structure.

In a second stage, an attempt was made to construct a general model containing 4 shells including a shell of fluorine atoms at ca. 3.5 Å. This structural model (table 1) is in close agreement with that proposed for the solid solution $Ca_{0.9}Ln_{0.1}F_{2.1}$ (Ln = La–Tm) [23]. As far as the first shell is concerned, the above model could be successfully applied to all other compositions. The number of fluorine atoms was fixed at 9 and the mean distance of the fluorine atoms to the uranium atom refined close to 2.30 ± 0.01 Å. On the other hand, the analysis of the second shell for all the compositions below $x=0.21$ was unsuccessful because of the lack of significant intensity of the EXAFS signal for the solid solutions featuring

Table 1
Structure parameters determined by EXAFS in $Ba_{0.95}U_{0.05}F_{2.10}$ (standard deviations in parentheses). The quality of the fit, as defined by $R=[\Sigma_k(\chi_{exp}-\chi_{calc})/\Sigma_k\chi^2_{exp}]$, $R=1.4\%$.

Shells	N	σ (Å)	R (Å)	ΔE_0 (eV)
F	9(1)	0.05(2)	2.30(1)	1.9(5)
F	3(1)	0.07(3)	3.51(2)	2.5(5)
Ba	7(1)	0.16(1)	4.38(2)	11(1)
U	4(1)	0.04(2)	4.38(2)	−6(1)

only low concentrations of uranium. However, for the compositions $x \geq 0.21$, curve fitting to the EXAFS of the second shell indicated the presence of a single uranium to metal distance, implying uranium to be located in barium atom sites at a distance (4.36 Å) entirely consistent with that expected in a fluorite-type lattice of unit cell parameter 6.12 Å. Furthermore, a much higher Debye–Waller factor (σ ca. 0.18 Å) is associated with the barium than with the uranium atoms (σ ca. 0.04 Å), indicative of a high disorder in the barium atom sub-lattice.

The results of this EXAFS spectroscopic study of six compositions in the phase diagram UF_4/BaF_2 are in disagreement with the conclusions drawn from diffuse neutron scattering [25,26] on the same system. On the other hand, these results are compatible with data obtained on the solid solutions $Ca_{0.9}Ln_{0.1}F_{2.1}$ [23] in the LnF_3/CaF_2 system with Ln=La–Tm, and $Ca_{0.68}Ln_{0.32}F_{2.32}$ [24] with Ln=Lu–Tb, using EXAFS spectroscopy. For example, the Ho–F distance observed in the solid solution $Ca_{0.68}Ho_{0.32}F_{2.32}$ using EXAFS is 2.27 Å, and 2.29 Å in HoF_3. However, a longer distance Ho–F of ca. 2.39 Å is expected in the fluorite type lattice of unit cell parameter $a=5.53$ Å [34]. This structural study thus demonstrated that the Ln–F distances found in these solid solutions were shorter than the distances expected in a regular fluorite lattice and very close to the Ln–F distances observed in LnF_3. However, according to these authors, a distinction can be made between the metal–metal distances Ca–Ln and Ln–Ln in the LnF_3/CaF_2 system whereas the results of our study in the UF_4/BaF_2 system, (as those of a recent neutron diffusion study [26]) show no difference between the distances U–Ba and U–U.

4. Conclusion

It is today clearly established that solid solutions based upon BaF_2 and CaF_2 lattices are fluorine ion conductors. For a certain critical concentration $x=x_p$ (percolation threshold) and "enhanced ionic motion" mode of conduction has been suggested [38]. Our results show that the position of this threshold differs for each solid solution; x ca. 0.07 for the solid solution $Ba_{1-x}U_xF_{2+2x}$, x ca. 0.05 for $Ba_{1-x}Nd_xF_{2+x}$, and x ca. 0.10 for $Ca_{1-x}Nd_xF_{2+x}$. Moreover, the differences observed in the variation of the electrical properties with the composition for the various systems can suggest different association processes of the defects in these solid solutions. For the solid solution $Ba_{1-x}U_xF_{2+2x}$, the previous structural study using neutron diffraction [26] which led the authors to conclude the presence of a 2/2/2 cluster [18,19] is in disagreement with our results showing an environment about the uranium in the fluorite lattice very close to that in UF_4.

However, it is clear that the uranium atoms do not exist isolated in the solid solution but rather are associated in a cluster of 4 or 5 atoms. If our EXAFS study is unable to distinguish the differences between the surroundings of the uranium in the various compositions, the different FTs show a short distance order around the uranium atom lower for the solid solutions low in concentration ($x<0.14$) than for the solid solutions of high concentration in uranium. This short distance order linked with the great increase of the conductivity characteristic of the lowest concentration in uranium ($x<0.07$) shows that the most important modification in the structure of these solid solutions only occurs for the lowest concentration in dopant atom ($x<0.07$). The same interpretation can be made with the solid solution $Ba_{1-x}Nd_xF_{2+x}$ featuring nearly the same electrical properties as $Ba_{1-x}U_xF_{2+2x}$.

This work, as in other recent attempts [6,35,39–41] to correlate the structure of the solid solution to their electrical properties clearly show the complexity of these systems. The previous studies carried out by EXAFS spectroscopy [23] and by neutron diffraction [39] on the solid solution $Ca_{1-x}Nd_xF_{2+x}$, have led to different interpretations in terms of clusters: a 2/2/3 cluster in the EXAFS work and 1/0/3 in the neutron diffraction study respectively. How-

ever, the minimum (x ca. 0.03) observed in the conductivity–composition isotherm fig. 2, is certainly the sign of a structural particularity of this solid solution. Indeed, the great disorder in the structure of all these superionic materials may explain in part that the structural methods used in this investigation seem to lead to different results.

Acknowledgement

We thank the Science and Engineering Research Council (UK) for access to experimental stations at the Daresbury SRS. The authors acknowledge the stimulating discussions enjoyed with Professor Jacques Rozière throughout this study.

References

[1] J.M. Schoonman, L.B. Ebert, C.H. Hsieh and A. Huggins, J. Appl. Phys. 46 (1975) 2873.
[2] J.M. Reau, J. Portier, A. Levasseur, G. Villeneuve and M. Pouchard, Mat. Res. Bull. 13 (1978) 1415.
[3] J.M. Reau, A. Rhandour, S.F. Matar and P. Hagenmuller, Mat. Res. Bull. 55 (1984) 7.
[4] A. Rhandour, J.M. Reau, S.F. Matar and P. Hagenmuller, J. Chem. Solids 47 (1986) 587.
[5] P. Hagenmuller, J.M. Reau, C. Lucat, S.F. Matar and G. Villeneuve, Solid State Ionics 3/4 (1981) 341.
[6] J.M. Reau, M. El Omari, J. Senegas and P. Hagenmuller, Mat. Res. Bull. 24 (1989) 1441.
[7] J.M. Reau, C. Lucat, G. Campet, J. Portier and A. Hammou, J. Solid State Chem. 17 (1976) 123.
[8] A.K. Ivanov-Shits and N.I. Sorokin, Solid State Ionics 36 (1989) 7.
[9] R.A. Panhuyzen, A.F.M. Arts, K.E.D. Wapenaar and J. Schoonman, Solid State Ionics 5 (1981) 641.
[10] K.E.D. Wapenaar and J. Schoonman, Solid State Ionics 2 (1981) 253.
[11] K.E.D. Wapenaar, J.L. Van Koesveld and J. Schoonman, Solid State Ionics 2 (1981) 145.
[12] K.E.D. Wapenaar and J. Schoonman, Solid State Ionics 5 (1981) 637.
[13] J.M. Reau, S.B. Tian, A. Rhandour, S.F. Matar and P. Hagenmuller, Solid State Ionics 15 (1985) 217.
[14] A. Rhandour, J.M. Reau and P. Hagenmuller, J. Solid State Chem. 61 (1986) 197.
[15] J.E. Mariani, V. Trnovcova, M. Svanter, B.P. Sobolev and P.P. Fedorov, 7 Konf. Fyzikû, Praha, 24 05-14 (1981).
[16] M. Ouwerkerk, E.M. Kelder and J. Schoonman, Solid State Ionics 9/10 (1983) 531.
[17] B.T.M. Willis, Proc. Br. Ceram. Soc. 1 (1964) 9.
[18] B.T.M. Willis, Acta Crystallogr. A34 (1978) 88.
[19] B.T.M. Willis and R.G. Hazell, Acta Crystallogr. A36 (1980) 582.
[20] A.K. Cheetham, B.E.F. Fender and M.J. Cooper, J. Phys. C 4 (1971) 3107.
[21] C.R.A. Catlow, J. Phys. C 9 (1976) 1859.
[22] D.J. Oostra and H.W. Den Hartog, Phys. Rev. B29 (1984) 2423.
[23] C.R.A. Catlow, A.V. Chadwick, G.N. Greaves and L.M. Moroney, Nature 312 (1984) 601.
[24] J.P. Laval, A. Abaouz, B. Frit and A Le Bail, J. Solid State Chem. 85 (1990) 133.
[25] N.H. Andersen, K. Clausen and J.K. Kjems, Solid State Ionics 9/10 (1983) 543.
[26] M. Ouwerkerk, N.H. Andersen, F. Veldkamp and J. Schoonman, Solid State Ionics 18/19 (1986) 916.
[27] E.G. Ippolitov, N.G. Gogadze and B.M. Zhigarnovskii, Russ. J. Inorg. Chem. 15 (1970) 1729.
[28] R.W.M. D'Eye and I.F. Ferguson, J. Chem. Soc. (1959) 3401.
[29] E. Catalano and W. Wrenn, J. Crystal Growth 30 (1975) 54.
[30] B.P. Sobolev and N.L. Tkachenko, J. Less-Common Met. 85 (1982) 155.
[31] EXAFS pour le Mac, A. Michalowicz, in: Ecole CNRS Structures fines d'absorption X en Chimie, Garchy, eds. H. Dexpert, A. Michalowicz and M. Verdaguer, C.N.R.S. 3 (1988).
[32] W.H. Zachariasen, Acta Crystallogr. 2 (1949) 388.
[33] A.C. Larson, R.B. Roof, Jr and D.T. Cromer, Acta Crystallogr. 17 (1964) 555.
[34] O. Greis and M. Kieser, Z. Anorg. Allg. Chem. 479 (1981) 165.
[35] M. El Omari, J.M. Reau and J. Senegas, J. Solid State Chem. 87 (1990) 430.
[36] J. Schoonman and H.W. Den Hartog, Solid State Ionics 7 (1982) 9.
[37] P. Fedorov, T.M. Turkina, B.P. Sobolev, E. Mariani and M. Svanter, Solid State Ionics 6 (1982) 331.
[38] K.E.D. Wapenaar and J. Schoonman, J. Electrochem. Soc. 126 (1979) 667.
[39] J.M. Reau and P. Hagenmuller, Appl. Phys. A49 (1989) 3.
[40] J.M. Reau, M. El Omari, J. Senegas and P. Hagenmuller, Solid State Ionics 38 (1990) 123.
[41] J.M. Reau, J. Senegas, M. El Omari, J.P. Laval and B. Frit, Phys. Status Solidi (a)117 (1990) 409.